5542 *Inorg. Chem.* **2010**, *49*, 5542–5545
DOI: 10.1021/ic100357q

Inorganic Chemistry
Article

Observation of Magnetic Ordering for Layered (2-D) Potassium Diruthenium Tetracarbonate, $K_3[Ru^{II/III}{}_2(O_2CO)_4]$: A Rare Second Row Transition Metal-based Magnet

Bretni S. Kennon and Joel S. Miller*

Department of Chemistry, 315 S. 1400 E. RM 2124, University of Utah, Salt Lake City, Utah 84112-0850

Received February 22, 2010

The detailed magnetic behavior of $K_3[Ru_2(CO_3)_4] \cdot xH_2O$ ($x = 2$) reveals that it has a 2-K magnetization at 5 T of 11 125 emu Oe/mol, a 50-Oe coercive field, and a remnant magnetization of 670 emu Oe/mol. It magnetically orders as a canted ferrimagnet below 4.2 K, and is a rare example of a magnetically ordered material based on a second row transition metal. The magnetic ordering confirms that the $S \neq 0$ M(II) site that bridges the layers in previously reported $H_xK_{1-x}M^{II}-[Ru^{II/III}{}_2(CO_3)_4](H_2O)_y(MeOH)_z$ (M = Mn, Fe, Co, Ni, Cu, Mg) does not contribute to the magnetic behavior that leads to magnetic ordering.

Introduction

The use of a D_{4h} paddlewheel-structured dimeric ruthenium species as a molecular building block to develop new molecule-based magnets possessing hexacyanometalates has led to new materials and extended structures in two and three dimensions.[1,2] Initial studies focused on the diruthenium tetracarboxylate cation, $[Ru_2(O_2CR)_4]^+$,[1,3,4] because (1) it has an $S = 3/2$ ground state with the $\sigma^2\pi^4\delta^2\delta^{*1}\pi^{*2}$ valence electronic configuration, due to near degeneracy of the π^* and δ^* orbitals,[5] and an unusually large zero-field splitting, D,[5b,6,7] and (2) each Ru is pentacoordinate, and thus able to coordinate to an additional ligand that is essential for constructing extended network structures. Various structural motifs can be obtained depending on the nature of the bridging carboxylate ligand. For example, acetate forms 3-D interpenetrating structures,[1b,c] while pivalate (O_2C^tBu) forms 2-D layered motifs with $[Cr(CN)_6]^{3-}$.[1a] In addition to cationic Ru_2-carboxylates, anionic Ru_2-based species are known,[8−10] and their study may lead to additional structural motifs and possibly contribute to a better understanding of magnetic behavior.

Recent work has shown that $[Ru^{II/III}{}_2(CO_3)_4]^{3-}$ is also a building block for magnetic materials, as it forms an extended network structure of $H_xK_{1-x}M^{II}[Ru^{II/III}{}_2(CO_3)_4](H_2O)_y(MeOH)_z$ (M = Mn, Fe, Co, Ni, Cu, Mg) composition that magnetically orders .[2a,c] They all magnetically order as canted ferrimagnets with $T_c = 4.4 \pm 1.0$ K, and the presence of $S = 0$ M^{II} = Mg(II) has essentially no effect on T_c, suggesting that the main magnetic pathway only occurs via four μ_3-$CO_3{}^{2-}$ (**I**) linkages within the layers, Figure 1a,

---

*To whom correspondence should be addressed. E-mail: jsmiller@chem.utah.edu.

[1] (a) Vos, T. E.; Miller, J. S *Angew. Chem., Int. Ed.* **2005**, *44*, 2416. (b) Vos, T. E.; Liao, Y.; Shum, W. W.; Her, J.-H.; Stephens, P. W.; Reiff, W. M.; Miller, J. S. *J. Am. Chem. Soc.* **2004**, *126*, 11630. (c) Liao, Y.; Shum, W. W.; Miller, J. S. *J. Am. Chem. Soc.* **2002**, *124*, 9336.

[2] (a) Kennon, B. S.; Her, J.-H.; Stephens, P. W.; Miller, J. S. *Inorg. Chem.* **2009**, *48*, 6117. (b) Her, J.-H.; Kennon, B. S.; Shum, W. W.; Stephens, P. W.; Miller, J. S. *Inorg. Chim. Acta* **2008**, *361*, 3462. (c) Kennon, B. S.; Her, J.-H.; Stephens, P. W.; Shum, W. W.; Miller, J. S. *Inorg. Chem.* **2007**, *46*, 9033.

[3] (a) Aquino, M. A. S. *Coord. Chem. Rev.* **1998**, *170*, 141. (b) Buslaeva, T. M.; Redkina, S. N.; Rudnitskaya, O. V. *Russ. J. Coord. Chem.* **1999**, *25*, 3. (c) Aquino, M. A. S. *Coord. Chem. Rev.* **2004**, *248*, 1025.

[4] Yoshioka, D.; Mikuriya, M.; Handa, M. *Chem. Lett.* **2002**, *31*, 1044.

[5] (a) Cotton, F. A.; Walton, R. A. In *Multiple Bonds between Metal Atoms*, 2nd ed.; Clarendon Press: Oxford, U.K., 1993; p 18. (b) Miskowiski, V. M.; Hopkins, M. D.; Winkler, J. R.; Gray, H. B. In *Inorganic Electronic Structure and Spectroscopy*; Solomon, E. I.; Lever, A. B. P., Eds.; John Wiley & Sons: New York, 1999; Vol. *2*, Chapter 6. (c) Norman, J. G., Jr.; Renzoni, G. E.; Case, D. A. *J. Am. Chem. Soc.* **1979**, *101*, 5256.

[6] (a) Telser, J.; Drago, R. S. *Inorg. Chem.* **1985**, *24*, 4765. (b) Telser, J.; Drago, R. S. *Inorg. Chem.* **1984**, *23*, 3114. (c) Cukiernik, F. D.; Giroud-Godquin, A. M.; Maldivi, P.; Marchon, J. C. *Inorg. Chim. Acta* **1994**, *215*, 203. (d) Handa, M.; Sayama, Y.; Mikuriya, M.; Nukada, R.; Hiromitsu, I.; Kasuga, K. *Bull. Chem. Soc. Jpn.* **1998**, *71*, 119. (e) Jimenez-Apraricio, R.; Urbanos, F. A.; Arrieta, J. M. *Inorg. Chem.* **2001**, *40*, 613.

[7] Cukiernik, F. D.; Luneau, D.; Marchon, J. C.; Maldivi, P. *Inorg. Chem.* **1998**, *37*, 3698.

[8] (a) Cotton, F. A.; Labella, L.; Shang, M. *Inorg. Chem.* **1992**, *31*, 2385. (b) Linday, A. J.; Wilkinson, G.; Motevalli, M.; Hursthouse, M. B. *J. Chem. Soc. Dalt.* **1987**, *11*, 2723. Yi, X.-Y.; Zheng, L.-M.; Xu, W.; Feng, S. *Inorg. Chem.* **2003**, *42*, 2827. Liu, B.; Li, Y.-Z.; Zheng, L.-M. *Inorg. Chem.* **2005**, *44*, 6921. Yi, X.-Y.; Liu, B.; Jiménez-Aparicio, R.; Urbanos, F. A.; Gao, S.; Xu, W.; Chen, J.-S.; Song, Y.; Zheng, L.-M. *Inorg. Chem.* **2005**, *44*, 4309. Liu, B.; Yin, P.; Yi, X.-Y.; Gao, S.; Zheng, L.-M. *Inorg. Chem.* **2006**, *45*, 4205. Liu, B.; Li, B.-L.; Li, Y.-Z.; Chen, Y.; Bao, S.-S.; Zheng, L.-M. *Inorg. Chem.* **2007**, *46*, 8524.

[9] McCann, M.; Murphy, E.; Cardin, C.; Convery, M. *Polyhedron* **1993**, *12*, 1725.

[10] Zhilyaev, A. N.; Fomina, T. A.; Kuz’menko, I. V.; Rotov, A. V.; Baranovski, I. B. *Russ. J. Inorg. Chem.* **1989**, *34*, 532. Kuz'menko, I. V.; Zhilyaev, A. N.; Fomina, T. A.; Porai-Koshits, M. A.; Baranovski, I. B. *Russ. J. Inorg. Chem.* **1989**, *34*, 1457. Cotton, F. A.; Datta, T.; Labella, L.; Shang, M. *Inorg. Chim. Acta* **1993**, *203*, 55.

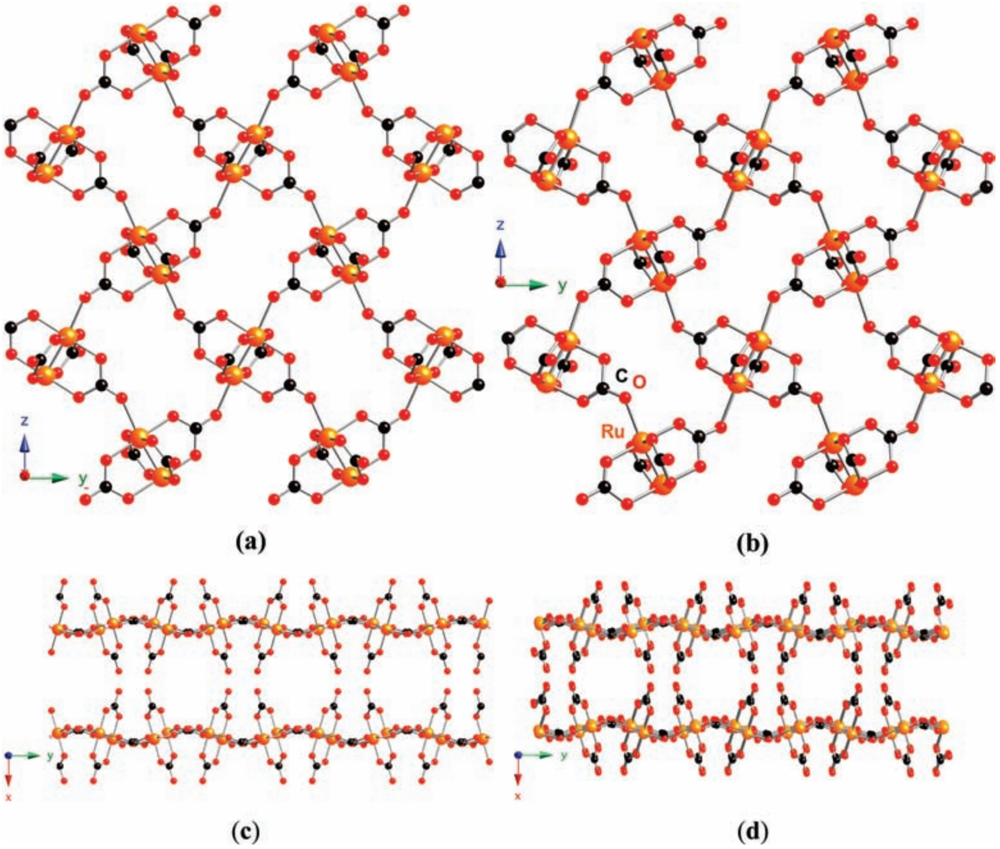

Figure 1. (a,b) Normal (*yz* plane) and (c,d) side (*xy* plane) views of the structure of a layer of $[M^{II}[Ru_2(CO_3)_4]^{-}$[2a,c] (a,c) and $K_3[Ru_2(CO_3)_4]$ (b,d),[8a] respectively. The cations have been omitted from the side views. Each structure has four type-**I** μ_3-CO_3^{2-} linkages.

separated by 9.25 ± 0.15 Å (*a*/2), and not via the M^{II}-based linkages that interconnect these layers.

The structure of $K_3[Ru^{II/III}{}_2(CO_3)_4]\cdot xH_2O$ consists of parallel layers of $[Ru_2(CO_3)_4]^{3-}$ [8.7 Å (*a*/2)] possessing four μ_3-CO_3^{2-} (**I**) linkages,[8a] Figure 1b, that are very similar to the layers present for $[M^{II}[Ru_2(CO_3)_4]^{-}$, Figure 1a, and as this is the dominant magnetic exchange pathway, the structure suggests that $K_3[Ru^{II/III}{}_2(CO_3)_4]\cdot xH_2O$ should also order as a canted ferrimagnet with a T_c in the vicinity of 4 K. To test this hypothesis, we report the detailed low temperature magnetic behavior of $K_3[Ru^{II/III}{}_2(CO_3)_4]$ (**1**). A previous investigation revealed that **1** has a χT value of 2.1 emu Oe/mol at room temperature in solution,[8b] but its temperature dependence of susceptibility in the solid state has yet to be reported.

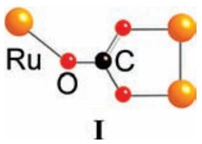

I

Experimental Section

$K_3[Ru_2(CO_3)_4]\cdot xH_2O$ was prepared via a literature route,[8a] and *x* was determined to be 2 from thermogravimetric analyses (TGA) obtained on a TA Model Q500 TGA. Its magnetic susceptibility was measured in an 1000 Oe applied field between 2 and 300 K on a Quantum Design (QD) MPMS superconducting quantum interference device (SQUID) equipped with a reciprocating sample measurement system, low field option, and continuous low temperature control with enhanced thermometry features, as previously described.[11] Powder samples for magnetic measurements were loaded into gelatin capsules. The temperature dependence of the DC magnetization was obtained by cooling in zero applied field, and then the data were collected on warming in a 5 Oe applied magnetic field. Hysteresis loops, a zero field, 5-Oe field-cooled conditions, remanent magnetizations, and AC susceptibilities measured at 10, 100, and 1000 Hz were obtained on a 9-T QD PPMS. In addition to correcting for the diamagnetic contribution from the sample holder, oxygen, and iron impurities, the core diamagnetic correction of -229×10^{-6} emu/mol for the dihydrate was used for analyzing the magnetic data. Thermogravimetric analysis (TGA) was performed at a scan rate of 5 °C/min under a continuous 10-mL/min N_2 flow using a TGA 2050 TA Instruments apparatus located in a Vacuum Atmospheres DriLab under nitrogen to protect air- and moisture-sensitive samples.

Results and Discussion

Upon the basis of the magnetic ordering observed for $H^+{}_xK^+{}_{1-x}M^{2+}[Ru^{II/III}{}_2(CO_3)_4]^{3-}(H_2O)_y(MeOH)_z$,[1a,b] and the close similarity of the its layered structure with $K_3[Ru_2(CO_3)_4]\cdot 4H_2O$ (**1**),[8a] the temperature dependence of the magnetic properties of **1** were determined to ascertain if magnetic ordering occurs. The magnetic susceptibility, χ, of **1** is plotted as $\chi T(T)$ and $\chi^{-1}(T)$, Figure 2. The 300 K χT value is 2.30 emuK/mol, and $\chi T(T)$ gradually decreased upon cooling and reached a minimum at ~26 K, and upon further

---

[11] Brandon, E. J.; Rittenberg, D. K.; Arif, A. M.; Miller, J. S. *Inorg. Chem.* **1998**, *37*, 3376.

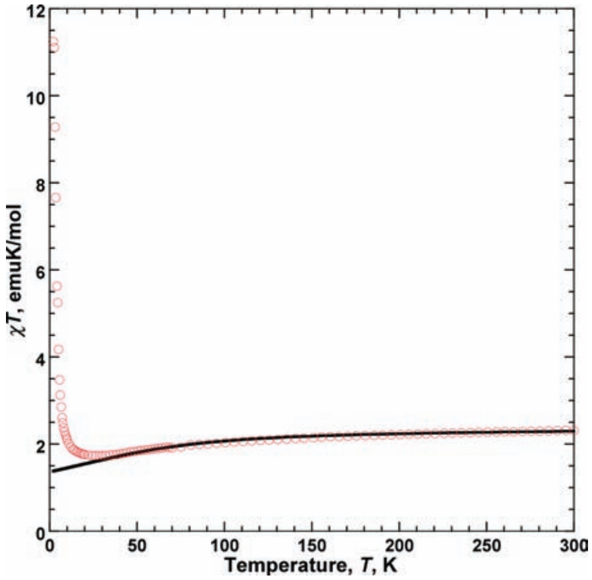

Figure 2. $\chi T(T)$ (○) with fit for the high-temperature data to eq 1 (solid line) for $K_3[Ru_2(CO_3)_4]\cdot 2H_2O$ (**1**).

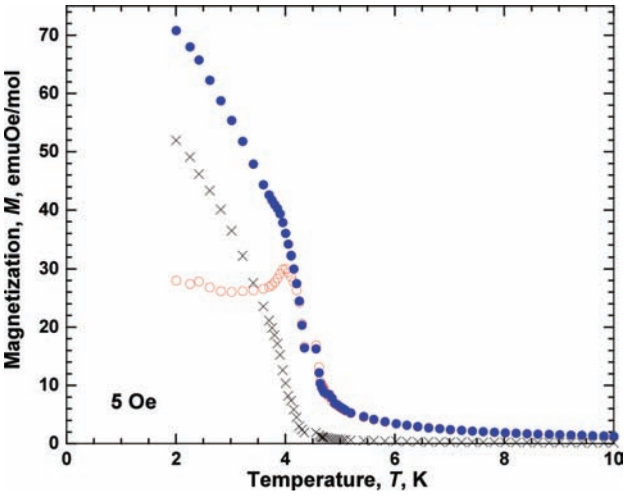

Figure 3. The 5-Oe $M(T)_{ZFC}$ (●), $M(T)_{FC}$ (○), and $M_r(T)$ (×) for **1**.

cooling $\chi T(T)$ rapidly increased. The gradual decrease below 300 K is attributed to the large zero field splitting (D) associated with the anion.[5b] Above 50 K, $\chi T(T)$ can be fit to an expression, eq 1, that accounts for D, as established for related Ru_2 compounds where N is Avogadro's number, k_B is Boltzmann's constant, μ_B is the Bohr magneton, g is the Landé g value, and TIP is the temperature independent paramagnetism.[6a,b] The Weiss constant, θ, is also introduced to account for intermolecular magnetic interactions. Above 50 K, the $\chi T(T)$ data are fit to eq 1 with $D/k_B = 100$ K, $g_{Ru2} = 2.2$, $\theta = 0$, and TIP is 200×10^{-6} emu/mol. The D and g values are in accord with previously reported values for related materials.[1,5,6c,d,7]

$$\chi = \frac{Ng_{Ru_2}^2\mu_B^2}{k_B(T-\theta)}\left[\frac{1}{3}\times\frac{1+9\,e^{-2D/k_BT}}{4(1+e^{-2D/k_BT})}+\frac{2}{3}\times\frac{1+\frac{3k_BT}{4D}(1-e^{-2D/k_BT})}{1+e^{-2D/k_BT}}\right]$$

$$+\frac{Ng_{M(II)}^2\mu_B^2(S)(S+1)}{3k_B(T-\theta)}+\text{TIP} \qquad (1)$$

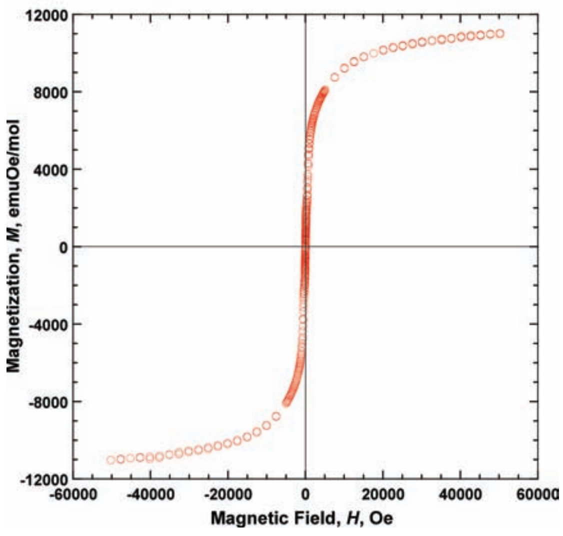

Figure 4. The 2 K $M(H)$ for **1**.

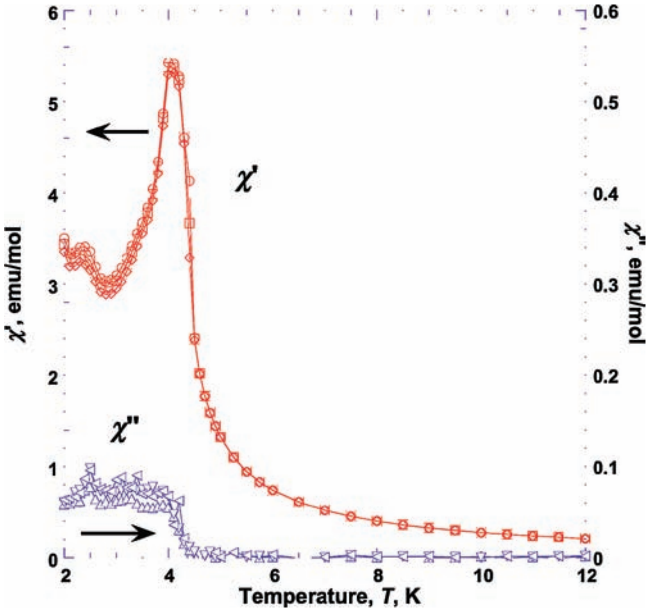

Figure 5. In-phase, $\chi'(T)$, and out-of phase, $\chi''(T)$, ac susceptibility data for **1**.

The zero-field cooled (ZFC) and field-cooled (FC) magnetizations, $M(T)_{ZFC}$ and $M(T)_{FC}$, respectively, for **1** rise sharply below 5 K (Figure 3), indicative of a magnetic transition. These data have a bifurcation temperature (T_b) of 4.2 K, while the extrapolated intercept of the $M(T)_{FC}$ data is 4.6 K. Likewise, extrapolation of the initial rise of the temperature-dependent remnant magnetization, $M_r(T)$, upon cooling gives an intercept of 4.3 K (Figure 3).

The magnetization at 5 T approaches saturation and is 11 125 emu Oe/mol for **1** (Figure 4). This is slightly greater than the expected value of 10 265 emu Oe/mol for the $S = 3/2$ species.[12] Hysteresis is observed in the 2 K $M(H)$ data with a coercive field of 50 Oe, (Figure 4), and the remnant magnetization, M_{rem}, is 670 emuOe/mol for **1**, which is characteristic of magnetic ordering.

---

[12] These values are reduced by 6400 emuOe/mol when the zero field splitting (D) is taken into account: Shum, W. W.; Liao, Y.; Miller, J. S. *J. Phys. Chem. A* **2004**, *108*, 7460.

Above 50 K, the susceptibility is due to the single ion paramagnetism; however, the rapid rise at low temperatures indicates magnetic ordering (Figure 2). Magnetic ordering was further established from the temperature and frequency dependent in-phase, $\chi'(T)$, and out-of phase, $\chi''(T)$, ac susceptibility studies, Figure 5. Frequency-independent absorptions are exhibited in both the $\chi'(T)$ and $\chi''(T)$ data; hence, **1** magnetically orders, as is also reported for H_xK_{1-x}-$M^{II}-(OH_2)_4[Ru_2(CO_3)_4]\cdot zH_2O$ (M = Mg, Mn, Fe, Co, Ni, Cu).[1b]

The magnetic ordering temperature is determined by the peak in the 10 Hz $\chi'(T)$ data and is 4.0 K. Alternatively, the T_c can be taken as the rise in $\chi''(T)$, and when the remanent magnetization, $M_{rem}(T)$, Figure 3, approaches zero, and these methods give comparable values of 4.2 and 4.3 K, respectively.

Conclusion

$K_3[Ru_2(CO_3)_4]$ is a rare example of a magnet based solely upon a second row transition metal and confirms the premise that the M(II) site present in $H_xK_{1-x}M^{II}[Ru^{II/III}{}_2(CO_3)_4]$-$(H_2O)_y(MeOH)_z$ (M = Mn, Fe, Co, Ni, Cu, Mg) and that bridges the layers does not contribute to the magnetic behavior that leads to magnetic ordering. The 4.2 K T_c exceeds the 3.5 ± 0.1 K reported for $H_{0.3}K_{0.7}Mg[Ru_2(CO_3)_4]$-$(H_2O)_3$[2a] and $Mn^{II}[Ru^{III}(acac)(CN)_2]$ (acac = acetylaetonate).[13] Other ruthenium-containing magnetic materials include $Ln_2M^{IV}{}_2O_7$ (Ln = rare earth, M = Ru, Ir) pyrochlores,[14] and the ferromagnetic cuprate superconductor $RuSr_2GdCu_2O_8$.[15]

Acknowledgment. The authors gratefully acknowledge the helpful discussions with William W. Shum and Amber C. McConnell, and the support from the NSF (Grant No. 0553573).

---

(13) Yeung, W.-F.; Man, W.-L.; Wong, W.-T.; Lau, T.-C.; Gao, S. *Angew. Chem., Int. Ed.* **2001**, *40*, 3031.

(14) Taira, N.; Wakeshima, M.; Hinatsu, Y. *J. Phys.: Condens. Matter* **1999**, *11*, 6983. Taira, N.; Wakeshima, M.; Hinatsu, Y. *J. Phys.: Condens. Matter* **2001**, *13*, 5527. (c) Taira, N.; Wakeshima, M.; Hinatsu, Y. *J. Mater. Chem.* **2002**, *12*, 1475.

(15) Malaughlin, A. C.; Janowitz, V.; MaAllister, J. A.; Attflied, J. P. *Chem. Commun* **2000**, 1331. Malaughlin, A. C.; Janowitz, V.; MaAllister, J. A.; Attflied, J. P. *J. Mater. Chem.* **2001**, *11*, 173.